

Anisotropic Thermal Expansion and Phase Transition in  $\text{Sc}_2(\text{MoO}_4)_3$ 

Koichiro FUKUDA

Department of Materials Science and Engineering, Nagoya Institute of Technology, Gokiso-cho, Showa-ku, Nagoya-shi 466-8555

 $\text{Sc}_2(\text{MoO}_4)_3$  の異方性熱膨張と相転移

福田功一郎

名古屋工業大学材料工学科, 466-8555 名古屋市昭和区御器所町

Lattice deformation in monoclinic  $\text{Sc}_2(\text{MoO}_4)_3$ , induced by both thermal expansion and phase transition, has been investigated by a matrix algebra analysis. From 4 K to 178 K, one of the principal distortions of the monoclinic lattice ( $\lambda_1$ ) invariably showed a positive coefficient of thermal expansion, while the other two distortions  $\lambda_2$  and  $\lambda_3$  showed negative thermal expansion in the temperature region of  $T < 55$  K ( $\lambda_2$ ) and  $T < 35$  K ( $\lambda_3$ ). Because of the bidimensional shrinkage along the latter two axes, volumetric contraction occurred below 30 K. The  $\lambda_2$ -axis coincides with the crystallographic  $b$ -axis. The intersection angle between the  $\lambda_1$ -axis and the crystallographic  $c$ -axis was  $\sim 78.8^\circ$  at 11 K, and it steadily decreased to  $\sim 20.1^\circ$  with increasing temperature up to 178 K. The magnitude of lattice deformation nearly along  $[302]$  is negligibly small. Therefore, the lattice deformation induced by the monoclinic-to-orthorhombic phase transition at 178 K was accompanied essentially by bidimensional expansion along  $[010]$  and nearly along  $[205]$ , the magnitudes of which are, respectively,  $\sim 0.6$  and  $\sim 0.9\%$ .

[Received May 11, 2001; Accepted August 9, 2001]

**Key-words:** Negative thermal expansion, Phase transition, Monoclinic, Anisotropy

## 1. Introduction

When a crystal is uniformly heated, it homogeneously deforms and uniformly expands. Because the crystals, except for the cubic system, are anisotropic, the thermal deformation depends on direction. If the initial crystal is spherical in shape, the resulting crystal after heating will be ellipsoidal. There are three directions perpendicular to each other along which the expansion is, respectively, a maximum, intermediate or minimum.<sup>1,2)</sup> These three mutually perpendicular directions form the principal axes of the resulting ellipsoid.

With crystals belonging to the tetragonal, trigonal, hexagonal and orthorhombic systems, the principal axes of deformation are exactly parallel to the crystallographic axes. However, with crystals belonging to the monoclinic system, one of the principal axes is parallel to the monoclinic axis ( $b$ -axis for second setting), and the two others do not necessarily coincide with the crystallographic axes. Accordingly, the temperature dependence of the principal distortions would be indispensable for a comprehensive understanding of the thermal expansion behavior of monoclinic crystals. Both the magnitudes and directions of the principal distortions are readily determined from calculations based on matrix algebra analysis.<sup>3,4)</sup>

Several oxides have been recently reported to show negative, or very low, thermal expansion behavior.<sup>5–8)</sup> Evans and Mary<sup>5)</sup> have investigated the thermal expansion and monoclinic-to-orthorhombic phase transition of  $\text{Sc}_2(\text{MoO}_4)_3$  by diffractometry from 4 K to 300 K. Despite the great similarity of crystal structure between the two phases, the contributions of thermal expansion anisotropy have been in marked contrast to each other. Below 178 K  $\text{Sc}_2(\text{MoO}_4)_3$  was monoclinic (space group  $P2_1/a$ ). As long as the temperature was below 30 K, the monoclinic phase showed slight negative thermal expansion, while, above 30 K, it had a positive coefficient of thermal expansion. It underwent a displacive phase transition at 178 K and the resulting orthorhombic phase definitely had a negative coefficient of thermal expansion up to 300 K; the  $a$  and  $c$  parameters showed a negative coefficient of thermal expansion, and the  $b$  parameter showed a positive coefficient. The relative mag-

nitudes of these coefficients were such that the bulk volume steadily shrinks with increasing temperature.

In the present study, the thermal deformation anisotropy of the monoclinic phase has been evaluated by matrix algebra analysis to determine the temperature dependence of the principal distortions. A similar analytical procedure (i.e., the phenomenological analysis as used in displacive phase transitions) has been applied to the monoclinic-to-orthorhombic phase transition. A close relationship has been demonstrated between the principal distortions induced by the thermal expansion and those by the phase transition.

## 2. Theory

## 2.1 Anisotropic thermal expansion in a monoclinic crystal

The initial monoclinic crystal at  $T_0$  will be, when heated at higher temperature  $T$ , homogeneously distorted into the new monoclinic crystal. The homogeneous distortion is generally characterized by the existence of three mutually orthogonal directions known as the principal axes of distortion. They remain orthogonal to each other after the distortion. The directions and magnitudes of the principal distortions upon heating from  $T_0$  to  $T$  are, respectively, the eigenvectors and eigenvalues ( $\lambda_i$ ) of the following equation:<sup>3,4)</sup>

$$|\mathbf{G}(T) - \lambda_i^2 \mathbf{G}(T_0)| = 0 \quad (1)$$

where  $\mathbf{G}$  is the matrix for the monoclinic phase, which is given by

$$\mathbf{G}(T) = \begin{bmatrix} a_T^2 & 0 & a_T c_T \cos \beta_T \\ 0 & b_T^2 & 0 \\ a_T c_T \cos \beta_T & 0 & c_T^2 \end{bmatrix}$$

where  $a_T$ ,  $b_T$ ,  $c_T$  and  $\beta_T$  are the cell dimensions at  $T$ . In the orthonormal basis defined by the principal axes, the matrix ( $\mathbf{D}$ ), which represents the lattice deformation, takes the simple form as follows:

$$\mathbf{D} = \begin{bmatrix} \lambda_1 & 0 & 0 \\ 0 & \lambda_2 & 0 \\ 0 & 0 & \lambda_3 \end{bmatrix}.$$

## 2.2 Lattice deformation induced by the monoclinic-to-orthorhombic phase transition

We assume that, upon low-high transition, the monoclinic phase lattice is homogeneously distorted into the or-

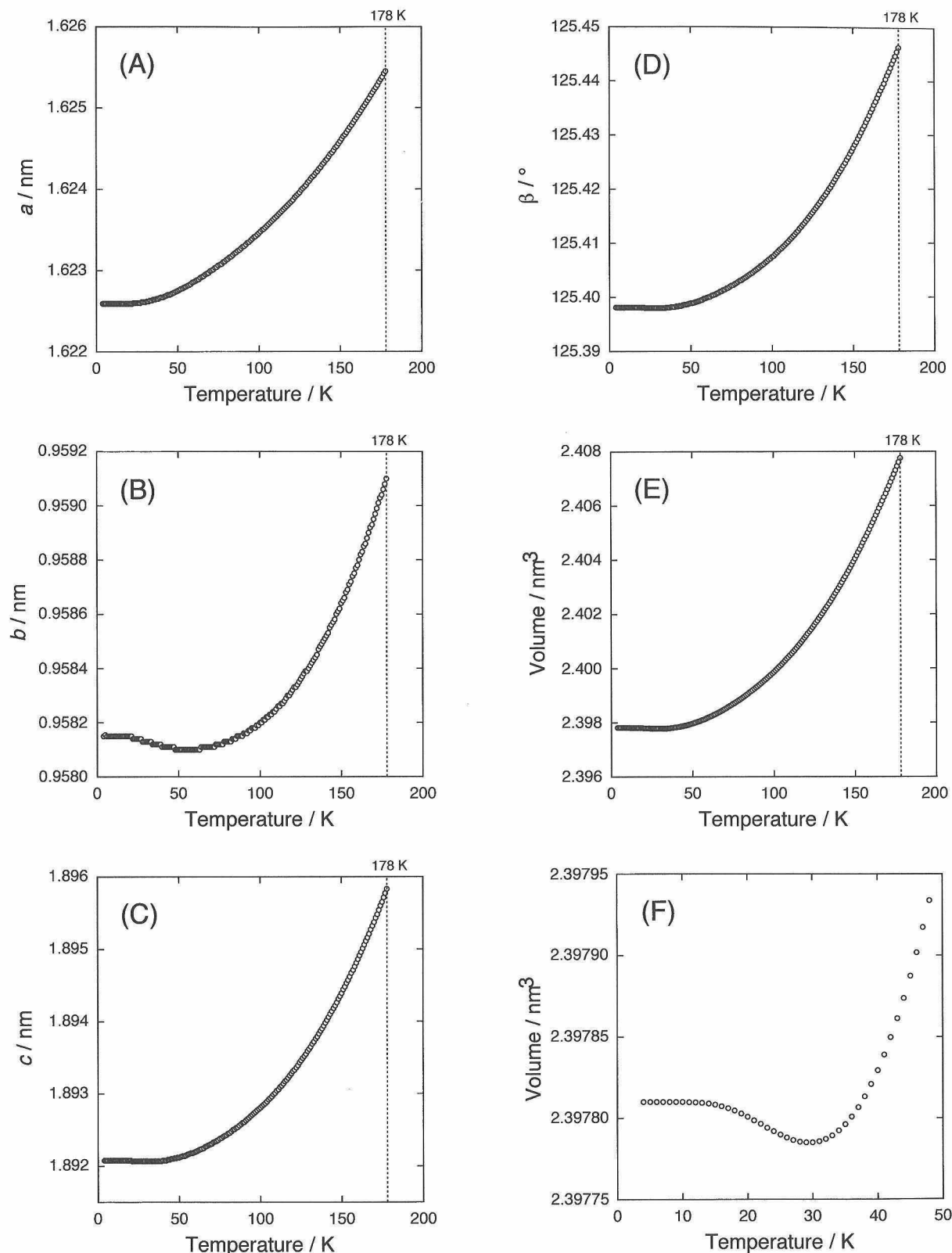


Fig. 1. Variation in unit-cell dimensions with temperature from 4 K to 178 K at 1 K intervals for monoclinic  $\text{Sc}_2(\text{MoO}_4)_3$  [(A)  $a$ , (B)  $b$ , (C)  $c$ , (D)  $\beta$ , (E) volume, and (F) enlargement of a part of the figure (E)]. The volume shrinks below 30 K. The dimensions determined from calculation based on the regression analysis by Evans and Mary.<sup>5)</sup>

thorhombic phase lattice. The magnitudes and directions of the principal distortions ( $\xi_i$ ) are given by the eigenvalues and eigenvectors of the following equation:<sup>9)-11)</sup>

$$|(\text{MC}'\text{O})(\text{O}^*\text{GO})(\text{OCM}) - \xi_i^2(\text{M}^*\text{GM})| = 0 \quad (2)$$

The matrix (OCM) represents the lattice correspondence between the monoclinic phase (M) and the orthorhombic phase (O). The matrix (MC'O) is the transpose of (OCM). The matrix (O\*GO) is for the orthorhombic phase and that

of (M\*GM) is for the monoclinic phase. Each metrix is determined from the individual cell dimensions at the transition temperature. In the orthonormal basis parallel to the principal axes, the lattice distortion matrix takes the simple form of a diagonal matrix, consisting of the three eigenvalues ( $\xi_1$ ,  $\xi_2$  and  $\xi_3$ ).

### 3. Results and discussion

#### 3.1 Change in cell dimensions of monoclinic $\text{Sc}_2(\text{MoO}_4)_3$ with temperature

Evans and Mary<sup>5)</sup> determined the temperature dependence of the cell dimensions for monoclinic  $\text{Sc}_2(\text{MoO}_4)_3$  from 4 K to 178 K. Based on the results of their regression analysis, we determined the cell dimensions by calculation at 1 K intervals, and plotted them as ordinate and the temperature as abscissa (Fig. 1). The  $b$ -axis showed negative thermal expansion below  $\sim 60$  K, and the  $a$ - and  $c$ -axes showed a zero or positive coefficient of thermal expansion above 4 K. These are in fair agreement with the experimental results.<sup>5)</sup>

Neither the magnitudes nor directions of the principal distortions, induced by thermal expansion, are currently available. Thus, it is still uncertain why the monoclinic phase was slightly negative below 30 K (Fig. 1(F)).

#### 3.2 Principal distortions ( $\lambda_i$ ) induced by thermal expansion in monoclinic $\text{Sc}_2(\text{MoO}_4)_3$

We have determined the directions and magnitudes of the principal distortions upon heating from 4 K up to 178 K by solving the Eq. (1). The magnitudes, together with the volume change  $V/V_{4K} (= \lambda_1 \lambda_2 \lambda_3)$ , are plotted in Fig. 2. In the entire temperature ranges, the magnitudes of the principal distortions bore the relationship  $\lambda_1 > \lambda_3 > \lambda_2$ . The magnitude of  $\lambda_1$  steadily increased with increasing temperature; the  $\lambda_1$ -axis invariably had a positive coefficient of thermal expansion. On the other hand,  $\lambda_3$  as well as  $\lambda_2$ , the latter of which is parallel to the  $b$ -axis, showed negative thermal expansion in the temperature region of  $T < 35$  K for  $\lambda_3$  and  $T < 55$  K for  $\lambda_2$ . The relative magnitudes of these principal distortions are such that the volume showed negative thermal expansion below 30 K.

Orthorhombic  $\text{Sc}_2(\text{MoO}_4)_3$  exhibited bidimensional shrinkage with increasing temperature.<sup>5)</sup> This would essentially lead to the contraction in volume. The volumetric contraction of monoclinic  $\text{Sc}_2(\text{MoO}_4)_3$  below 30 K may be interpreted in the same way; the bidimensional shrinkage along  $\lambda_2$  and  $\lambda_3$  would be indispensable for the negative thermal expansion.

The  $\lambda_2$ -axis necessarily coincides with the crystallographic  $b$ -axis. The directions of  $\lambda_1$  and  $\lambda_3$  are simply represented by the acute angle  $\lambda_1 \wedge c$  (Fig. 3). With increasing temperature from 11 K to 178 K, the angle steadily decreased from  $\sim 78.8^\circ$  to  $\sim 20.1^\circ$  (Fig. 4). For example with the lattice

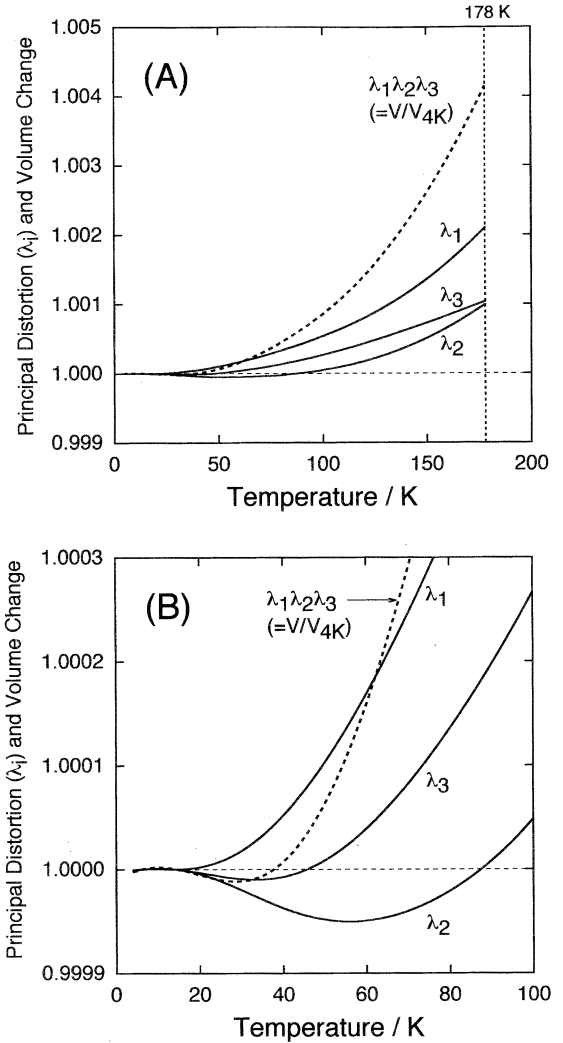


Fig. 2. Temperature dependence of principal distortions ( $\lambda_i$ ) and volume change ( $\lambda_1 \lambda_2 \lambda_3$ ). One of the distortions,  $\lambda_1$ , is almost invariably larger than unity, while the others,  $\lambda_2$  and  $\lambda_3$ , are less than unity below  $\sim 88$  K for the former and below  $\sim 45$  K for the latter. The relative magnitudes of the three distortions are such that, due to the contraction in both  $\lambda_2$  and  $\lambda_3$ , volumetric shrinkage occurs below  $\sim 30$  K.

deformation at 178 K, the directions of the three principal distortions, which are expressed in the orthonormal basis defined by the unit vectors  $i$ ,  $j$  and  $k$ , are given in Table 1.

Table 1. Principal Distortions ( $\lambda_i$ ) of Monoclinic  $\text{Sc}_2(\text{MoO}_4)_3$  upon Heating from 4 to 178 K

$\lambda_1$	$\lambda_2$	$\lambda_3$
$ \lambda_1  = 1.0021$	$ \lambda_2  = 1.0010$	$ \lambda_3  = 1.0010$
$\lambda_1 = -0.3432i + 0.9393k$	$\lambda_2 = j$	$\lambda_3 = -0.9393i - 0.3432k$

$i$ ,  $j$  and  $k$  are the unit vectors in the orthonormal basis defined by  $i \parallel a^*$ ,  $j \parallel b$  and  $k \parallel c$ .

$a$ ,  $b$  and  $c$  are crystallographic axes of the monoclinic cell at 4 K.

$\lambda_1$ ,  $\lambda_2$  and  $\lambda_3$  are the unit vectors along the principal axes.

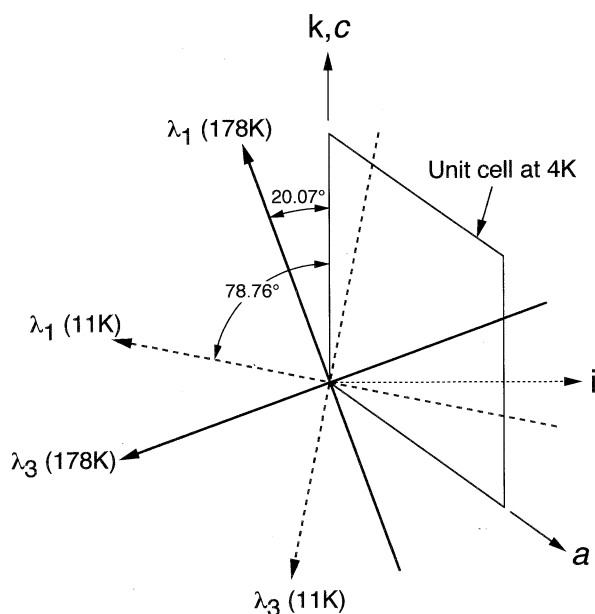


Fig. 3. Superposition of the principal axes  $\lambda_1$  and  $\lambda_3$  on the monoclinic unit cell at 4 K. The intersection angle  $\lambda_1 \wedge c$  is used to define the orientation of  $\lambda_1$  and  $\lambda_3$ . The  $\lambda_2$ -axis coincides with the  $b$ -axis. The  $\lambda_i$ (11 K) and  $\lambda_i$ (178 K) are the principal axes upon heating from 4 K to, respectively, 11 K and 178 K. The orthonormal basis defined by the unit vectors  $i$  ( $\parallel a^*$ ),  $j$  ( $\parallel b$ ) and  $k$  ( $\parallel c$ ).

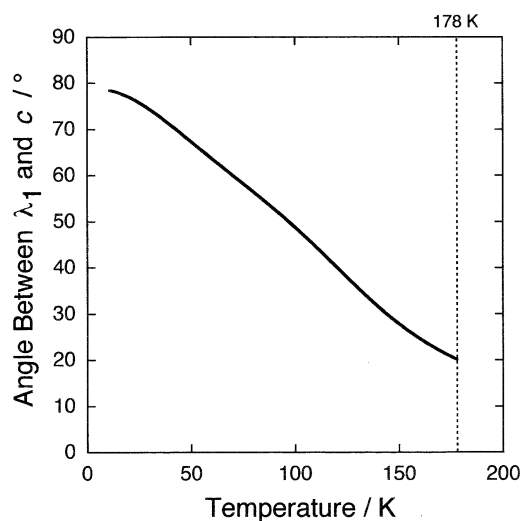


Fig. 4. Temperature dependence of the intersection angle  $\lambda_1 \wedge c$ , which defines the orientation of the principal axes  $\lambda_1$  and  $\lambda_3$ . The angle steadily decreases from  $\sim 78.8^\circ$  to  $\sim 20.1^\circ$  with increasing temperature from 11 K to 178 K.

The magnitudes of the relevant principal distortions indicate that the initial lattice at 4 K expands in all directions when heated at 178 K. The maximum expansion of  $\sim 0.2\%$  occurred along the  $\lambda_1$ -axis. Both expansion magnitudes along the other principal axes  $\lambda_2$  and  $\lambda_3$  were  $\sim 0.1\%$ . During subsequent heating, the monoclinic-to-orthorhombic phase transition, as mentioned below, will immediately occur.

### 3.3 Principal distortions ( $\xi_i$ ) induced by the monoclinic-to-orthorhombic phase transition

The cell parameters of the monoclinic phase at the transition temperature (178 K) are given in Table 2. With the orthorhombic phase, we have determined the cell parameters at 178 K by linear extrapolation; this calculation is based on the cell parameters at 200 K and the coefficients of linear thermal expansion along the  $a$ -,  $b$ - and  $c$ -axes, all of which are given by Evans and Mary.<sup>5)</sup> The matrix representing the lattice correspondence between the two phases (OCM) is given by

$$(\text{OCM}) = \begin{bmatrix} 0 & \bar{1} & 0 \\ \bar{1} & 0 & 0 \\ 1 & 0 & \bar{2} \end{bmatrix}$$

Equation (2) has been solved with the cell parameters and the lattice correspondence to determine the magnitudes and directions of the three principal distortions (Table 3). One of the principal distortions  $\xi_3$  was very close to unity, and the others were larger than unity. This implies that the lattice deformation upon low-high transition is such that, assuming  $\xi_3 = 1$ , bidimensional expansion essentially occurs along the  $\xi_1$ - and  $\xi_2$ -axes, the magnitudes of which are  $\sim 0.9\%$  for the former and  $\sim 0.6\%$  for the latter.

The direction of  $\xi_1$ , together with that of  $\xi_3$ , is superimposed on the schematic diagram of the monoclinic unit cell at 178 K (Fig. 5). The  $\xi_1$ -axis and  $c$ -axis intersect at an angle of  $\sim 12.60^\circ$ . Thus, the directions of  $\xi_1$  and  $\xi_3$  are, respectively, nearly parallel to  $[205]$  and  $[302]$  of monoclinic  $\text{Sc}_2(\text{MoO}_4)_3$  ( $\xi_1 \wedge [205] = \sim 0.52^\circ$  and  $\xi_3 \wedge [302] = \sim 1.03^\circ$ ). Since the lattice deformation along  $[302]$  is negligibly small, the structural change before and after the transition could be clearly demonstrated by the atomic arrangements when viewed along  $[302]$ , which corresponds to  $[031]$  of the orthorhombic phase.

The monoclinic-to-orthorhombic phase transition occurs as the result of the thermal deformation of the monoclinic phase during heating. Comparing the principal distortions induced by the thermal expansion at 178 K ( $\lambda_i$ (178 K)) and those by the phase transition ( $\xi_i$ ) shows there is little difference in orientation; the intersection angle between  $\lambda_1$ (178 K) and  $\xi_1$  is only  $7.47^\circ$  ( $= 20.07^\circ - 12.60^\circ$ ). In addition, the  $\lambda_1$ (178 K) is, among the three distortions of  $\lambda_i$ (178 K), the largest in magnitude, and so is the  $\xi_1$ . Accordingly, it may be concluded that there is a close relationship in both magnitude and orientation between  $\lambda_i$ (178 K) and  $\xi_i$ . Detailed clarification of this relationship as well as of the negative thermal expansion mechanism is a subject for the future. In this respect, a comparative investigation of the monoclinic and orthorhombic structures at around 178 K would en-

Table 2. Cell Parameters of the Monoclinic and Orthorhombic  $\text{Sc}_2(\text{MoO}_4)_3$  at 178 K

Crystal System	$a$ (nm)	$b$ (nm)	$c$ (nm)	$\beta$ ( $^\circ$ )	Volume (nm <sup>3</sup> )
Monoclinic	1.62545	0.95910	1.89583	125.446	2.4078
Orthorhombic	0.96485	1.32367	0.95564	—	1.2205

Table 3. Principal Distortions ( $\xi_i$ ) and Volume Change ( $\xi_1\xi_2\xi_3$ ) upon Monoclinic-to-Orthorhombic Lattice Deformation at 178 K

Principal distortions			Volume change
$\xi_1$	$\xi_2$	$\xi_3$	$\xi_1\xi_2\xi_3$
$ \xi_1  = 1.0086$	$ \xi_2  = 1.0060$	$ \xi_3  = 0.9992 (\approx 1)$	1.014
$\xi_1 = -0.2182\mathbf{i} + 0.9759\mathbf{k}$	$\xi_2 = \mathbf{j}$	$\xi_3 = -0.9759\mathbf{i} - 0.2182\mathbf{k}$	

$\mathbf{i}$ ,  $\mathbf{j}$  and  $\mathbf{k}$  are the unit vectors in the orthonormal basis defined by  $\mathbf{i} \parallel a^*$ ,  $\mathbf{j} \parallel b$  and  $\mathbf{k} \parallel c$ .

$a$ ,  $b$  and  $c$  are crystallographic axes of the monoclinic cell at 178 K.

$\xi_1$ ,  $\xi_2$  and  $\xi_3$  are the unit vectors along the principal axes.

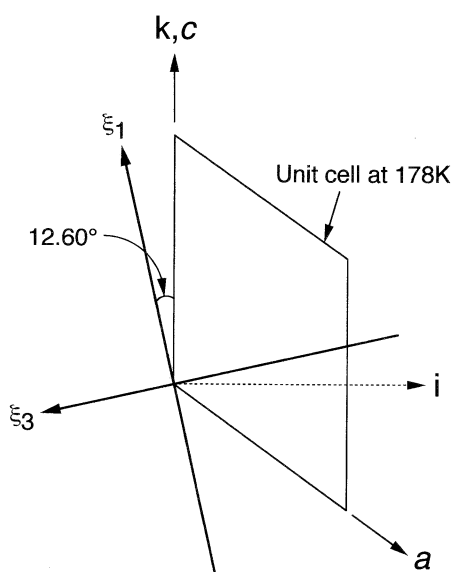


Fig. 5. Superposition of the principal axes  $\xi_1$  and  $\xi_3$  on the monoclinic unit cell at 178 K. The  $\xi_2$ -axis coincides with the  $b$ -axis. The orthonormal basis defined by the unit vectors  $\mathbf{i}$  ( $\parallel a^*$ ),  $\mathbf{j}$  ( $\parallel b$ ) and  $\mathbf{k}$  ( $\parallel c$ ).

hance our understanding of the unusual thermal behavior of  $\text{Sc}_2(\text{MoO}_4)_3$ .

#### 4. Conclusions

(1) With thermal expansion of monoclinic  $\text{Sc}_2(\text{MoO}_4)_3$ , one of the principal distortions  $\lambda_1$  was invariably larger than unity; the magnitude steadily increased with increasing temperature. The other distortions,  $\lambda_2$  and  $\lambda_3$ , showed negative thermal expansion in the temperature region of  $T < 55$  K for  $\lambda_2$  and  $T < 35$  K for  $\lambda_3$ . Because of the bidimensional shrink-

age along the latter two axes, volumetric contraction occurred below 30 K.

(2) The  $\lambda_2$ -axis coincides with the crystallographic  $b$ -axis. The intersection angle between  $\lambda_1$  and  $c$  was  $\sim 78.8^\circ$  at 11 K; it steadily decreased to  $\sim 20.1^\circ$  with increasing temperature to 178 K.

(3) The lattice deformation, induced by the monoclinic-to-orthorhombic phase transition at 178 K, was essentially accompanied by the bidimensional expansion along  $[010]$  and nearly along  $[\bar{2}05]$ , the magnitudes of which are respectively  $\sim 0.6$  and  $\sim 0.9\%$ .

(4) Since the lattice deformation along  $[\bar{3}0\bar{2}]$  is negligibly small, the structural change before and after the transition could be clearly demonstrated when viewed along  $[\bar{3}0\bar{2}]$ , which corresponds to  $[031]$  of the orthorhombic phase.

#### References

- 1) Zhdanov, G. S., "Crystal Physics," Oliver & Boyd Press, Edinburgh (1965).
- 2) Nye, J. F., "Physical Properties of Crystals," The Clarendon Press, Oxford (1957).
- 3) Christian, J. W., "The Theory of Transformations in Metals and Alloys," Pergamon Press, Oxford, U.K. (1975).
- 4) Fukuda, K., Maki, I. and Ito, S., *J. Am. Ceram. Soc.*, **80**, 1595–98 (1997).
- 5) Evans, J. S. O. and Mary, T. A., *Int. J. Inorg. Mat.*, **2**, 143–51 (2000).
- 6) Mary, T. A., Evans, J. S. O., Sleight, A. W. and Vogt, T., *Science*, **272**, 90–92 (1996).
- 7) Evans, J. S. O., Mary, T. A., Vogt, T., Subramanian, M. A. and Sleight, A. W., *Chem. Mater.*, **8**, 2809–23 (1996).
- 8) Evans, J. S. O., Mary, T. A. and Sleight, A. W., *Physica B*, **241–243**, 311–16 (1998).
- 9) Wayman, C. M., "Introduction to the Crystallography of Martensitic Transformations," The Macmillan Company, New York (1964).
- 10) Fukuda, K., *J. Mater. Res.*, **14**, 460–64 (1999).
- 11) Fukuda, K., *J. Ceram. Soc. Japan*, **108**, 701–04 (2000).